

Magnetic enhancement of pure gamma Fe_2O_3 nanochains by chemical vapor deposition

This article has been downloaded from IOPscience. Please scroll down to see the full text article.

2008 J. Phys.: Condens. Matter 20 075217

(<http://iopscience.iop.org/0953-8984/20/7/075217>)

View [the table of contents for this issue](#), or go to the [journal homepage](#) for more

Download details:

IP Address: 129.252.86.83

The article was downloaded on 29/05/2010 at 10:34

Please note that [terms and conditions apply](#).

Magnetic enhancement of pure gamma Fe₂O₃ nanochains by chemical vapor deposition

Shao-Min Zhou¹, Xing-Tang Zhang, He-Chun Gong, Bin Zhang, Zhi-Shen Wu, Zu-Liang Du and Si-Xin Wu

Key Laboratory for Special Functional Materials, Henan University, Kaifeng 475004, People's Republic of China

E-mail: smzhou@henu.edu.cn

Received 20 September 2007, in final form 14 November 2007

Published 28 January 2008

Online at stacks.iop.org/JPhysCM/20/075217

Abstract

High-yield pure chain-like one-dimensional nanostructures consisting of single-crystal γ -Fe₂O₃ nanoparticles have been produced by using a chemical vapor deposition (CVD) approach. The constituents, phase, and magnetic properties of these nanochains have been determined. The synthesized nanochains can be reorganized under a weak magnetic field (about 0.4 T). The nanochain growth mechanism is proposed to be driven by magnetostatic interaction. The hysteresis loop was operated to show that the magnetic properties of the nanochains are strongly influenced by the morphology of the crystal. Room temperature magnetic measurements show that the as-fabricated γ -Fe₂O₃ nanochains are ferromagnetic with higher saturation magnetization and higher coercivity values than those of the counterpart bulk, which could have potential applications in spin filtering, high-density magnetic recording and nanosensors.

1. Introduction

In the past decade, magnetic nanomaterials have attracted much attention due to their physical properties and technological applications [1–32]. Among these materials, maghemite (γ -Fe₂O₃) is superior to others because of its high chemical inactivity (in contrast to that of commonly used pure Fe metal), excellent properties for magnetic recording media, magnetic anisotropy, and superparamagnetic effects, which are crucial for device applications [2–30]. In addition, maghemite has proven to be a ferromagnetic material with a high spin polarization at the Fermi level, which results in a semiconductor majority spin channel and a metallic minority spin channel. Faraday effects in maghemite samples have been analyzed taking into account the in-plane optical anisotropy, and such a composite material is a promising candidate for future magneto-optical applications [4]. Since Whitney *et al* reported the fabrication and magnetic properties of arrays of metallic nanowires, where arrays of ferromagnetic nanowires were fabricated by electrochemical deposition and had enhanced coercivities as

high as 680 Oe and remnant magnetization up to 90% [1], iron based nanomaterials such as iron oxides have been synthesized in external organic or inorganic containers [2–31] and intensively characterized with special emphasis on their structure and magnetic properties. However, the corresponding physical properties are inevitably affected by the external solid container. More recently, the magnetic anisotropy of epitaxial films of γ -Fe₂O₃ (001) composed entirely of Fe³⁺ [30], single-crystal γ -Fe₂O₃ nanowires [25], and nanotubes [27] has been reported. However, pure chain-like γ -ferric oxide nanochains have not been directly observed experimentally, although nanochains with organics and polymers have been studied experimentally and theoretically [10, 31, 32]. In this paper, we report the synthesis of pure γ -Fe₂O₃ nanochains by a simple CVD technique and determine their room temperature ferromagnetic properties with higher saturation magnetization and coercivity. The study of pure γ -Fe₂O₃ nanochains and their room temperature ferromagnetic properties is a key issue, not only for practical applications but also for fundamental understanding.

¹ Author to whom any correspondence should be addressed.

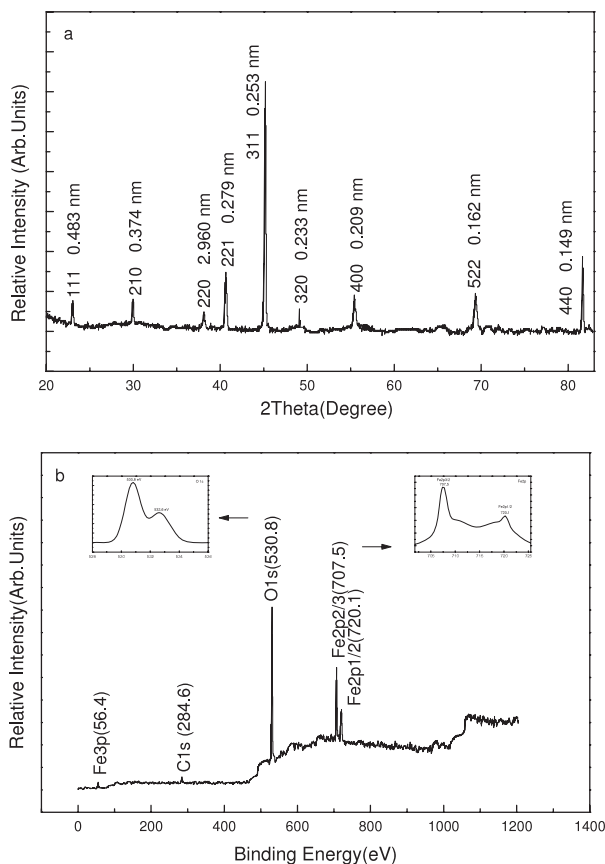


Figure 1. (a) XRD patterns of the collected product. (b) A typical full XPS spectrum of a γ -Fe₂O₃ sample with the high-resolution XPS spectrum of O 1s binding energy peaks at 530.8 and 532.6 eV (left) and the high-resolution XPS spectrum of Fe 2p at 707.5 and 720.1 eV (right).

2. Experimental details

In a typical experiment, a small quartz boat was first cleaned using a standard treatment in piranha solution (10% H₂O₂ + 20% H₂SO₄), and rinsed with deionized water. Iron nitrate powders (10.0 g) were placed in half of the boat, which was inserted into half of a large quartz-tube in a horizontal tube furnace. Then a quartz boat with a permanent-magnet material (~ 0.25 T) was put in a quarter of the furnace (lower temperature area) (this technique and set-up will be patented in China) and the system was quickly heated to 500 °C under a gas flow of 50 sccm oxygen gas at a pressure of about 10^{-3} Torr for 1 h. It was then cooled to room temperature. Subsequently, large-scale scarlet wool-like products were seen in the quartz boat.

The samples were characterized extensively for morphology, phase, chemical composition and magnetic properties using energy dispersive x-ray spectroscopy (EDS), x-ray powder diffraction (XRD), transmission electron microscopy (TEM), selective area electron diffraction (SAED), and x-ray photoelectron spectroscopy (XPS). The temperature dependence of magnetization was studied and a room temperature magnetic study carried out using a physical properties measurement system (Quantum Design PPMS-7).

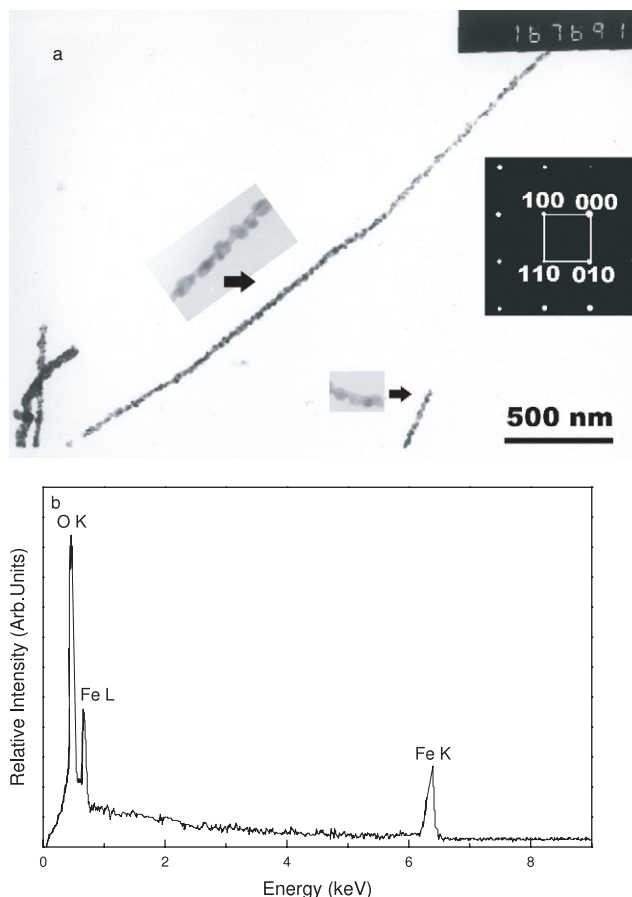


Figure 2. (a) A typical TEM image of one γ -Fe₂O₃ nanochain (left inset, greatly enlarged TEM image of the middle nanochain; lower inset, greatly enlarged TEM image of the end nanochain; right inset, corresponding SAED pattern). (b) A typical EDS pattern of the γ -Fe₂O₃ nanochains.

3. Results and discussion

Figure 1(a) shows a typical XRD pattern of bulk γ -Fe₂O₃ nanochain products where all of the diffraction peaks can be assigned to the FeO primitive cubic structure (P4232) ($a = 0.836$ nm) (see JCPDS-ICDD card no. 24-0081, June 2002) and no impurity phases such as iron nitrate or other oxides were detected within experimental error. More accurately, XPS was used to determine the composition of the bulk γ -Fe₂O₃ nanochain arrays samples as shown in figure 1(b). The XPS spectra contain a wide-scan XPS spectrum with high-resolution XPS spectra of O 1s (left) at 530.8 eV and 532.6 eV and Fe 2p (right) at 707.5 eV and 720.1 eV, respectively. According to the area of the peaks, the ratio of Fe to O in the nanochain is about 13:21, which may demonstrate that within experimental error a 2:3 Fe/O composition has been synthesized. As shown in figure 2(a), a typical TEM image is shown, in which highly dense uniform chain-like nanostructures can be seen and the diameter (about 50 nm) and length (up to several micrometers) of a single nanochain can be measured. Insets in figure 2(a) are two typical enlarged scale TEM images to show the morphologies of the nanoparticles and the junction parts of the nanochain (the

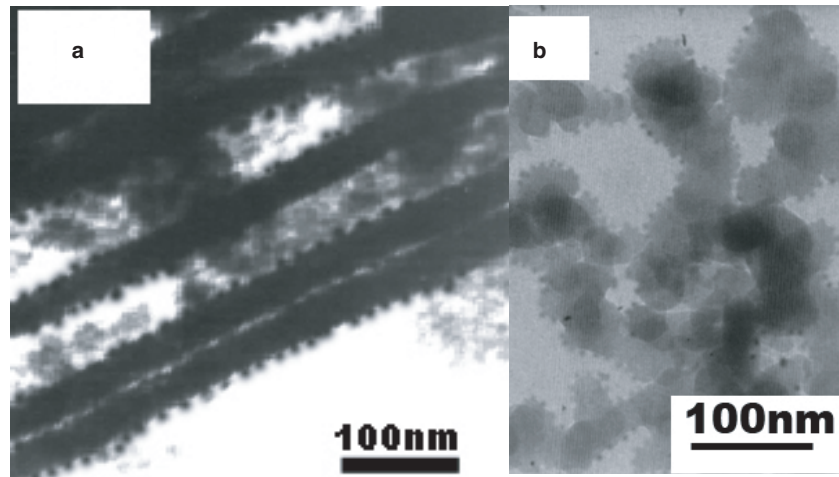


Figure 3. (a) Alignment of γ -Fe₂O₃ nanochains in a weak external magnetic field (about 0.4 T). (b) Non-alignment of γ -Fe₂O₃ nanochains without a magnetic field.

middle and lower side in figure 2(a)). From the TEM images, the chain-like array nanostructures are demonstrated. The right inset in figure 2(a) shows a typical SAED pattern, which can be indexed to the single-crystal cubic γ -Fe₂O₃ structure as indicated. Diffraction patterns taken from different parts of the nanochain axis show the same features, indicating the same periodic orientation along the single-crystalline γ -Fe₂O₃ nanochain. These diffraction dots can be indexed well by using the cubic γ -Fe₂O₃ with a lattice constant of $a = 0.836$ nm, in agreement with XRD results and earlier reports [25–27]. EDS analysis, as shown in figure 2(b), taken from the single nanochain in figure 2(a), indicates that the nanochain has the same composition and contains Fe and O. Further quantitative analysis of EDS finds that the atomic ratio of Fe:O is about 2:3, indicating that a stoichiometric nanochain (Fe/O = 2:3) is obtained and is consistent with stoichiometric Fe₂O₃, in agreement with the XPS results. The synthesized nanochains can be reorganized in a weak magnetic field (about 0.4 T). Typically, the purified γ -Fe₂O₃ nanochains were dispersed into deionized water by ultrasonic agitation. A drop of the nanochain solution was dripped on a holey copper grid with a carbon film to characterize the TEM in the presence of a weak external magnetic field (about 0.4 T) and dried naturally. The results reveals that the γ -Fe₂O₃ nanochains in the weak magnetic field have aligned according to the direction of the magnetic field as shown in figure 3(a), whereas without an external magnetic field non-aligned nanochains appear as shown in figure 3(b). Regarding the mechanism for the growth of highly branched γ -Fe₂O₃ nanoparticle chains, we believe that magnetostatic interaction plays an important role. The magnetic dipole–dipole interaction behaved like a soft template. Initially, very small γ -Fe₂O₃ nanoparticles were formed. With increasing growth time, presumably, the small γ -Fe₂O₃ nanoparticles diffused and aggregated to form larger nanoparticles. The larger γ -Fe₂O₃ nanoparticles were then assembled into necklace-like chains with multiple branches because of the stronger anisotropic magnetic forces.

In figure 4(a), the curves show the temperature dependence of magnetization for γ -Fe₂O₃ between 4 and 350 K using zero-field-cooling (ZFC) and field-cooling (FC) procedures under an applied magnetic field of 50 Oe. It is found that the blocking temperature of the γ -Fe₂O₃ nanochains is about 230 K. This result is larger than the blocking temperature of the γ -Fe₂O₃ nanowires reported in [8] (120 K) and [24] (200 K), which can be attributed to aligned nanochains because the blocking temperature increases with the increase of the particle size and degree of alignment [24]. The room temperature magnetic properties of the synthesized γ -Fe₂O₃ nanochains and γ -Fe₂O₃ conventional powders are presented in figure 4(b). It can be clearly seen that the synthesized nanochains have a larger saturation magnetization (106 emu g⁻¹) than conventional γ -Fe₂O₃ powders (38 emu g⁻¹) that we prepared and tested under the same conditions. The value of the coercivity amounts to 120 Oe for γ -Fe₂O₃ nanochains, which is larger than that of conventional γ -Fe₂O₃ powders (62 Oe). It can be expected that the reduced size and dimensionality of the γ -Fe₂O₃ nanostructures may change the magnetization reversal mechanism, leading to a large enhancement of coercivity, which is similar to what has been found in previous works [1–30]. As shown in figure 4(c), the γ -Fe₂O₃ nanochains exhibit a superparamagnetic behavior and no coercivity or remanence is observed at 340 K. Compared with those γ -Fe₂O₃ nanoparticles reported [≤ 200 K] [28, 29], blocking temperature of our aligned nanochains has a higher temperature at about 230 K.

4. Conclusions

The approach used in this study provides a simple and inexpensive method for the preparation of stable and magnetic γ -Fe₂O₃ nanochains. The as-synthesized nanochains are ferromagnetic at room temperature, which may have potential applications in biotechnology, biomedicine, and fundamental science. In addition, the present facile growth process is

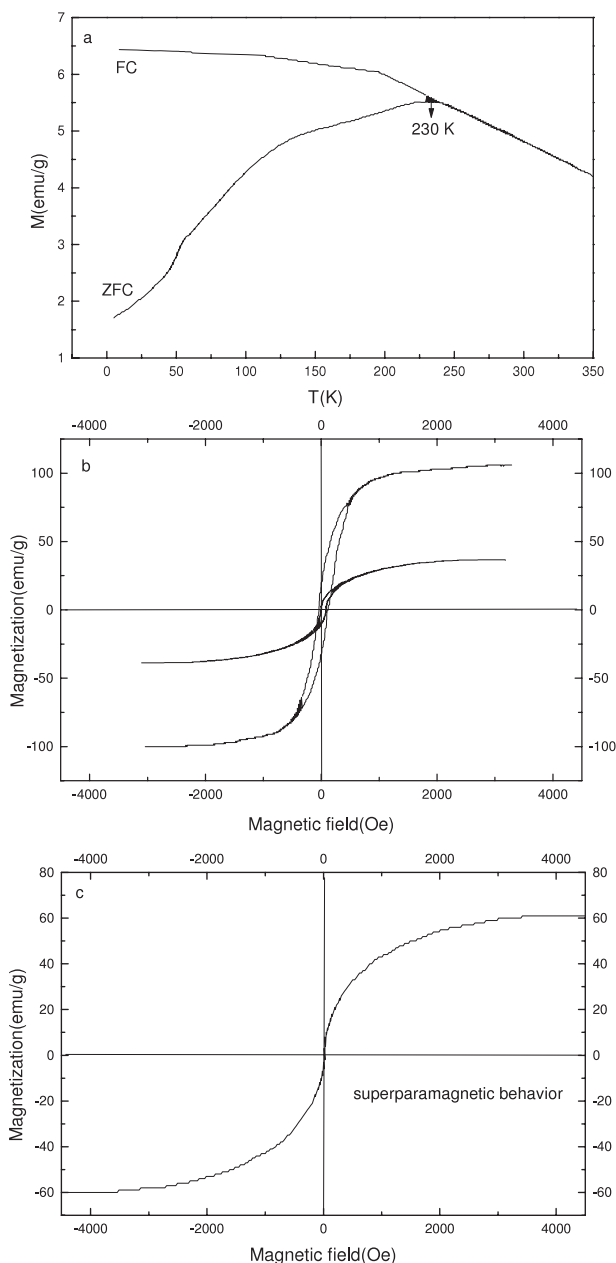


Figure 4. (a) Field cooled and zero field cooled magnetization curves of gamma oxide iron nanochains, measured in a field of 50 Oe. (b) Room temperature magnetic hysteresis curves of the synthesized γ -Fe₂O₃ nanochains and γ -Fe₂O₃ conventional powders with a fixed applied field of 4.5 kOe. (c) Superparamagnetic curve of the synthesized γ -Fe₂O₃ nanochains at 320 K with a fixed applied field of 4.5 kOe.

expected to be readily extendable to the fabrication of similar functional arrays of nanostructures of other metals.

Acknowledgments

This work was partially supported by the Ministry of Science and Technology of China (grant no. 2007cb616911). SMZ acknowledges financial support from the Science and Technology Innovation Talents in Universities of Henan Province (HASTIT) and the Hunan Provincial Natural Science

Foundation of China (project no. 06jj5120) and Academician Shuit-Tong Lee (City University of Hong Kong) for helpful discussions.

References

- [1] Whitney T, Searson P, Jiang J and Chien C 1993 *Science* **261** 1316
- [2] Prodan D, Chaneac C, Tronc E, Jolivet J, Cherkaour R, Ezzir A, Nogues M and Dormann J 1999 *J. Magn. Magn. Mater.* **203** 63
- [3] Morales M, Veintemillas-Verdaguer S and Serna C 1999 *J. Mater. Res.* **14** 3066
- [4] Bentivegna F, Nyvlt M, Ferre J, Jamet J, Brun A, Visnovsky S and Urban R 1999 *J. Appl. Phys.* **85** 2270
- [5] Yan X, Liu G, Liu F, Tang B, Peng H, Pakhomov A and Wong C 2001 *Angew. Chem. Int. Edn* **40** 3593
- [6] Shafi K, Ulman A, Dyal A, Yan X, Yang N, Estournes C, Fournes L, Wattiaux A, White H and Rafailovich M 2002 *Chem. Mater.* **14** 1778
- [7] Butter K, Bomans P, Frederik P, Vroege G and Philipse A 2003 *Nat. Mater.* **2** 88
- [8] Xiong Y, Xie Y, Li Z, Zhang R and Yang J 2003 *New J. Chem.* **27** 588
- [9] Jang J and Yoon H 2003 *Adv. Mater.* **15** 2088
- [10] Lalatonne Y, Richardi J and Pileni M 2004 *Nat. Mater.* **3** 121
- [11] Zhang L, Xue D, Xu X, Gui A and Gao C 2004 *J. Phys.:* *Condens. Matter* **16** 4541
- [12] Frandsen C, Rasmussen H and Morup S 2004 *J. Phys.:* *Condens. Matter* **16** 6977
- [13] Cheon J, Kang N, Lee S, Lee J, Yoon J and Oh S 2004 *J. Am. Chem. Soc.* **126** 1950
- [14] Wang J, Peng Z, Huang Y and Chen Q 2004 *J. Cryst. Growth.* **263** 616
- [15] Jia C, Sun L, Yan Z, You L, Luo F, Han X, Pang Y, Zhang Z and Yan C 2005 *Angew. Chem. Int. Edn* **44** 4328
- [16] Wiemann J, Dai J, Tang J, Long G and Spinu L 2005 *J. Appl. Phys.* **97** 2005
- [17] Wang D, Cao C, Xue S and Zhu H 2005 *J. Cryst. Growth.* **277** 238
- [18] Yang W, Lee C, Tang H, Shieh D and Yeh C 2006 *J. Phys. Chem. B* **110** 14087
- [19] Kim T, Rajan K and Shima M 2006 *IEEE Trans. Nanobiosci.* **5** 210
- [20] Zhong L, Hu J, Liang H, Cao A, Song W and Wan L 2006 *Adv. Mater.* **18** 2426
- [21] Lu J, Yang S, Ng K, Su C, Yeh C, Wu Y and Shieh D 2006 *Nanotechnology* **17** 5812
- [22] Yusuf S, De Teresa J, Mukadam M, Kohlbrecher J, Ibarra M, Arbiol J, Sharma P and Kulshreshtha S 2006 *Phys. Rev. B* **74** 224428
- [23] Wang Z and Zeng X 2006 *J. Wunan Univ. Technol.* **21** 28
- [24] Talapin D, Shevchenko E, Murray C, Titov A and Kral P 2007 *Nano Lett.* **7** 1213
- [25] Han Q, Liu Z, Xu Y, Chen Z, Wang T and Zhang H 2007 *J. Phys. Chem. C* **111** 5034
- [26] Niederberger M, Garnweitner G, Ba J, Polleux J and Pinna N 2007 *Int. J. Nanotechnol.* **4** 263
- [27] Jia C, Sun L, Yan Z, Pang Y, You L and Yan C 2007 *J. Phys. Chem. C* **111** 13022
- [28] Sreeja V and Joy P 2007 *Mater. Res. Bull.* **42** 1570
- [29] Zhu H, Yang D, Zhu L, Yang H, Jin D and Yao K 2007 *J. Mater. Sci.* **42** 9205
- [30] Yanagihara H, Hagiwara J, Nakazumi M, Kita E and Furubayashi T 2007 *Appl. Phys. Lett.* **91** 072508
- [31] Geng B, Ma J, Liu X, Du Q, Kong M and Zhang L 2007 *Appl. Phys. Lett.* **90** 043120
- [32] Tlusty T and Safran S 2000 *Science* **290** 1328